Electron relaxation times in high-carrier-density GaAs-(Ga,Al)As heterojunctions

R. M. Kusters,* F. A. Wittekamp, J. Singleton,† and J. A. A. J. Perenboom
High Field Magnet Laboratory, University of Nijmegen, NL-6525 ED Nijmegen, The Netherlands
and Research Institute for Materials, University of Nijmegen, NL-6525 ED Nijmegen, The Netherlands

G. A. C. Jones, D. A. Ritchie, and J. E. F. Frost
Cavendish Laboratory, University of Cambridge, Madingley Road, Cambridge CB3 0HE, United Kingdom

J.-P. André
Laboratoire d'Electronique et de Physique Appliquée, F-94450 Limeil-Brevannes, France
(Received 17 October 1991; revised manuscript received 15 April 1992)

From the amplitudes of the Shubnikov–de Haas (SdH) oscillations in magnetotransport measurements on different GaAs-(Ga,Al)As heterojunctions with two occupied subbands, the subband single-particle relaxation times have been extracted. The lowest-subband single-particle relaxation time appears to be modulated by the second-subband SdH oscillation periodicity, indicating the importance of screened long-range Coulomb scattering and nonlinear intersubband scattering. Parallel-field and near-parallel-field magnetoresistance measurements reveal that the presence of the second-subband electrons affects the lower-subband electrons in two different ways: the onset of intersubband scattering leads to a decrease of the transport scattering time in the lower subband, while the additional screening provided by the upper-subband electrons leads to an increase of the single-particle relaxation time.

I. INTRODUCTION

Recently interest has grown in high-carrier-density two-dimensional electron-gas (2DEG) systems in which more than one electric subband is populated.[1–6] These systems are not strictly two dimensional, as the presence of more than one populated subband is a manifestation of the third dimension, and the wave functions associated with the higher subbands will have a successively larger spread in the direction perpendicular to the plane of the 2DEG. Their electronic behavior is significantly more complicated than that of a system with only one occupied subband. The subbands cannot be treated as separate 2DEG's, especially at high fields. Interactions between the subbands appear to be important: intersubband scattering affects the scattering rates, and all carriers experience a potential that is screened by the carriers in both subbands. In high magnetic fields the highly degenerate Landau levels give rise to a field-dependent subband occupancy. As higher subbands extend further into the GaAs layer, the confinement potential of the heterojunction will depend on the subband occupations so that the subband separation E_{10} also becomes field dependent. Other quantities that show a self-consistently determined field-dependent behavior are the level broadening and the spin splitting.

In recent publications some controversy has arisen about the relation between transport mobilities and level broadening.[1–5] In most cases it has been found that the second-subband electrons have a lower mobility but a longer single-particle relaxation time than the lowest-subband electrons. This behavior is attributed to the predominance of long-range scattering by ionized impurities (donors) in the (Ga,Al)As layer of the heterostructure, screened by the 2DEG. In a swept-field experiment, where the filling factor is varied with the magnetic field, the screening depends on the position of the Fermi level relative to the Landau levels, and this leads to oscillations in the screening as a function of field with the same periodicities as the SdH oscillations.[7–9] In this paper we will show that in a two-subband system in high magnetic fields, the electrons in the lowest subband are subject to very strong screening by electrons in the second-subband's Landau levels. This screening is governed by the position of the Fermi energy relative to the Landau levels of both subbands, and can so be modulated by varying the applied magnetic field.

II. EXPERIMENT

We have performed an extensive series of high-field magnetotransport experiments on four different high-carrier-density GaAs-(Ga,Al)As heterojections. Samples 1, 2, and 3 were grown by molecular-beam epitaxy[10] (MBE): in these samples the (Ga,Al)As region is undoped, except for a monolayer containing 5×10^{16} m^{-2} Si atoms on Ga sites. The donors will be spread somewhat in the growth direction due to migration; the actual width of the doping layer depends on the growth temperature and is typically of the order of several nm.[11] The difference between the three MBE-grown samples is the position of this δ-doping layer. The three samples also have a superlattice buffer consisting of 21 AlAs barrier layers, 2.5 nm wide, and 20 GaAs wells of the same width. Sample 4 was grown by metal-organic chemical vapor deposition[12] (MOCVD) and is a conventional

TABLE I. Relevant sample parameters, SL indicates the presence of a 20×(2.5 nm GaAs + 2.5 nm AlAs) superlattice buffer.

Sample	1	2	3	4
μ_{dark} (m^2/Vs)	9.4	52	73	8.1
μ_{light} (m^2/Vs)	8.5	52	75	21.5
$N_{s,dark}$ (10^{15} m^{-2})	8.9	6.4	3.8	4.9
$N_{s,light}$ (10^{15} m^{-2})	16.6	11.6	6.6	8.8
Al content (%)	33	33	33	35
spacer (nm)	5	10	20	10
doped layer thickness (nm)	0.5	0.5	0.5	60
doping concentration (10^{16} m^{-2})	5	5	5	3×10^{23} m^{-3}
cap layer thickness (nm)	10	10	10	20
cap layer doping (10^{24} m^{-3} Si)	1.7	1.7	1.7	1.0
buffer thickness (μm)	1.0+SL	1.0+SL	1.0+SL	1.0

modulation-doped heterojunction.[13] The carrier densities, mobilities, and other relevant parameters are given in Table I. All samples have been patterned into Hall bars. AuGeNi contacts have been made on the side arms of the Hall bars and at the ends.

Magnetoresistance and Hall resistance were measured using conventional techniques in either a helium bath cryostat or a dilution refrigerator. The helium bath cryostat contained a rotation stage, allowing the sample to be rotated through an angle of 360° in the field, with a precision of 0.1°. Temperatures used in this cryostat were ~1.2 K. The magnetic field was supplied by a 20 T Bitter magnet. In all measurements great care was taken to avoid hot-electron effects due to excessive sample currents.[14] During all measurements the carrier density of the 2DEG could be varied by controlled light doses from a red light-emitting diode ($\hbar\omega > E_g$); this variation is due to the persistent photoconductivity effect.[15]

III. EXPERIMENTAL RESULTS

A. Electron densities of the subbands

In Fig. 1 the subband carrier densities N_0 and N_1 are shown as a function of 2DEG sheet density N_s for each of the four samples. These results are compared to densities calculated self-consistently by Ando at two different fixed densities of the depletion charge.[16] We see the following general trend: the second subband is not noticeably occupied until a certain threshold value of N_s; just above this threshold, N_1 tends to increase much more steeply than the theoretical curves do, but soon afterwards the slope of the N_1 versus N_s plot levels off until it is about the same as the slopes of the theoretical curves. This behavior can be explained by a light-induced decrease of the depletion charge, which is self-limiting. Before illumination the depletion charge has a density sufficient to prevent population of the second subband at the 2DEG carrier density. On illumination of the sample the depletion charge decreases due to the formation of electron-hole pairs in the GaAs, which are separated by the depletion field,[4,17] and this will lead to a steeper dependence of N_1 on N_s than given in Ando's model for fixed N_{depl}. As the depletion field decreases a situation will be reached in which this field cannot separate the electron-hole pairs created by the radiation anymore, i.e., the decrease of the depletion charge is self-limiting. N_{depl} will reach a constant level[18] and cause the experimental N_1 versus N_s curve to become approximately parallel to the theoretical curves. The high N_s part of the curves suggests a rather low depletion charge.[17]

We have studied the depopulation of the second subband[19,20] using parallel-field magnetoresistance measurements. The depopulation fields have been extracted from the inflection points of the magnetoresistance curves,[21,22] and the results are shown as a function of carrier density N_s in Fig. 2. After some illumination of the samples with red light ($\hbar\omega > E_g$), there is good agreement between our experimental data and the model of Reisinger and

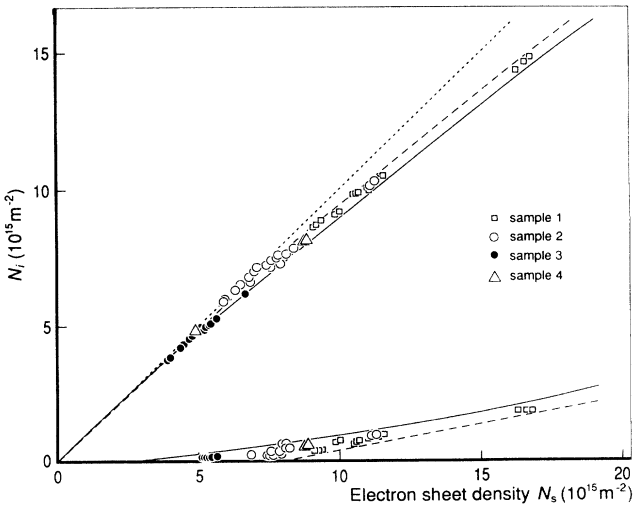

FIG. 1. Subband carrier densities N_0 and N_1 vs total 2DEG carrier density N_s measured on samples 1–4. The subband carrier densities calculated in Ref. 16 for different values of the depletion charge density N_{depl} are given by the lines. The Solid line for $N_{depl}=1\times10^{13}$ m^{-2}, the dashed line for $N_{depl}=5\times10^{14}$ m^{-2}. The dotted line represents the case of zero higher-subband occupancy $N_0=N_s$.

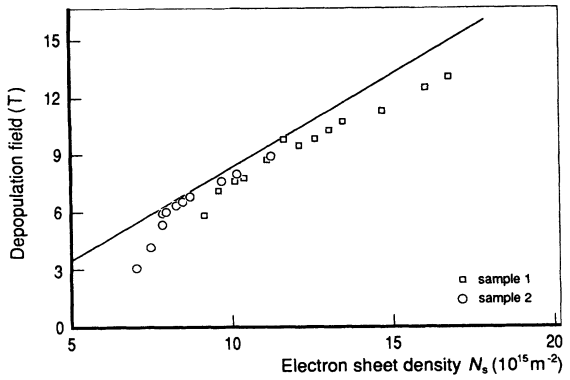

FIG. 2. Depopulation field values extracted from the inflection points of the depopulation curves for samples 1 and 2. The solid line represents the model of Reisinger and Koch.[19]

Koch,[19] indicating accumulation-layer-like behavior of these samples (see Fig. 2). For sample 2 (and more weakly for sample 1) there is a clear deviation of the data from the curve at the onset of population of the second subband; this further supports our interpretation based on the illumination-induced self-limiting decrease of the depletion charge that is complete at $N_s \approx 8\times10^{15}$ m^{-2} for sample 2 and $N_s \approx 9.5\times10^{15}$ m^{-2} for sample 1. The slight misfit at larger N_s is probably due to parallel conduction in these samples after strong illumination.

B. Landau-level broadening in perpendicular field

In the relaxation-time approximation[23,24] the mobility of the carriers is related to a transport scattering time τ_t by

$$\mu=\frac{e\tau_t}{m^*} . \tag{1}$$

However, in a magnetic field many electronic properties also depend on the broadening of Landau levels, which determines the density of states. The density of states at the Fermi level in turn determines most thermodynamic quantities. The Gaussian broadening of the Landau levels is related to the single-particle relaxation time τ_S by

$$\Gamma=\frac{\hbar}{\tau_S} , \tag{2}$$

where Γ is the full width at half maximum.

The relations between various scattering mechanisms and the lifetimes are given by[2,25,26]

$$\frac{1}{\tau_t}=\int d\mathbf{k}'P(\mathbf{k},\mathbf{k}')(1-\cos\theta) , \tag{3}$$

$$\frac{1}{\tau_S}=\int d\mathbf{k}'P(\mathbf{k},\mathbf{k}') , \tag{4}$$

where $P(\mathbf{k},\mathbf{k}')$ is the total probability of scattering from state $\mathbf{k}$ into state $\mathbf{k}'$ due to all scattering mechanisms, and θ is the scattering angle.

The transport scattering times τ_{t0} and τ_{t1} of the electrons in the lowest and the second-subband respectively, can be determined from the low-field classical magnetoresistance.[1] The single-particle relaxation times τ_{S0} and τ_{S1} can be extracted from the field dependence of the amplitudes of the SdH oscillations due to the Landau levels of the respective subbands. It often happens that the slow oscillations arising from the second subband are visible down to much lower fields so that τ_{S1} can be obtained in a range of lower fields than τ_{S0}. If this is not the case the oscillations in the average of the top and bottom envelopes of the SdH oscillations due to the lowest subband must be taken into account.

The oscillatory part of the magnetoresistance is given by[26,27]

$$\frac{\tilde{\rho}}{\rho_0}=2\sum_{s=1}^{\infty}\frac{sX}{\sinh(sX)}\exp\left[\frac{-\pi s}{\omega_c\tau_S}\right]\cos\left[\frac{2\pi sE_F}{\hbar\omega_c}-s\pi\right] , \tag{5}$$

where $\tilde{\rho}(B)$ is the amplitude of the SdH oscillation at field B, ρ_0 is the zero-field resistivity, and $X=2\pi^2k_BT/\hbar\omega_c$. $D(sX)=sX/\sinh(sX)$ represents the thermal damping of the oscillations. In the low-field regime it is sufficient to retain only the first term $s=1$ of the series expansion, due to the factor $\exp(-\pi s/\omega_c\tau_S)$. The oscillatory part of ρ_{xx} has been evaluated at its minima; as E_F is an integer times $\hbar\omega_c$ the cosine term has the value -1. The single-particle relaxation time is extracted from the slope of the Dingle plot, i.e., a plot of $\ln[\tilde{\rho}/2\rho_0D(X)]$ versus $1/B$.

It should be noted that this τ_S is related to the thermodynamic density of states that is affected by inhomogeneous level broadening. The electron dephasing time (i.e., the time that an electron can be considered as existing in a single-particle momentum eigenstate), however, is related to the homogeneous broadening, which is probed by low-field cyclotron resonance measurements.[28]

A typical example of a set of Dingle plots from data obtained on sample 2 is shown in Fig. 3; the upper part shows data corresponding to the lowest subband, the middle part shows data corresponding to the second subband, and the lower part shows a Dingle plot of the same sample at a density at which no second-subband occupation could be observed. The lower and the upper parts of Fig. 3 show a distinct difference: the Dingle plot taken when the second subband was occupied shows some oscillations with the periodicity of the second-subband SdH oscillations, while the Dingle plot taken with only lowest-subband occupation shows an approximately straight line. Similar plots taken from all MBE-grown samples show oscillations that grow in strength as the second-subband population increases.

In Fig. 4 an example of a $\tau_{S0}(1/B)$ plot is shown for sample 1, plotted as $\mu_q=e\tau_{S0}/m_0^*$. This plot has been calculated using Eq. (5). It clearly shows a modulation of τ_{S0} at the second-subband fundamental frequency; the amplitude of this intermodulation decreases with inverse field (Landau-level index). This behavior is expected: at lower fields the Landau levels are less well resolved and oscillations in the screening and hence the intersubband scattering rate (see below) become weaker.

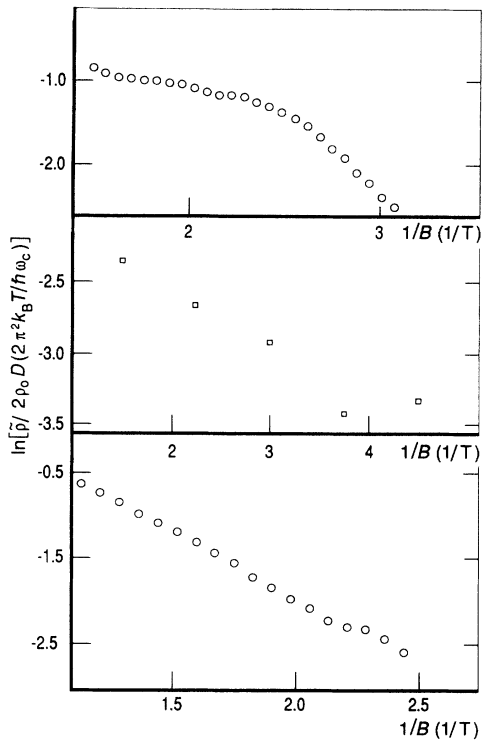

FIG. 3. Typical set of Dingle plots, with data from sample 2. The upper two parts are the lowest-subband and second-subband Dingle plots, respectively, extracted from the same SdH trace; the subband carrier densities are $N_0=7.40\times10^{15}$ m^{-2} and $N_1=0.32\times10^{15}$ m^{-2}. The lower plot has been extracted from measurements on the same sample in a situation where only the lowest subband was occupied: $N_0=N_s=6.36\times10^{15}$ m^{-2}.

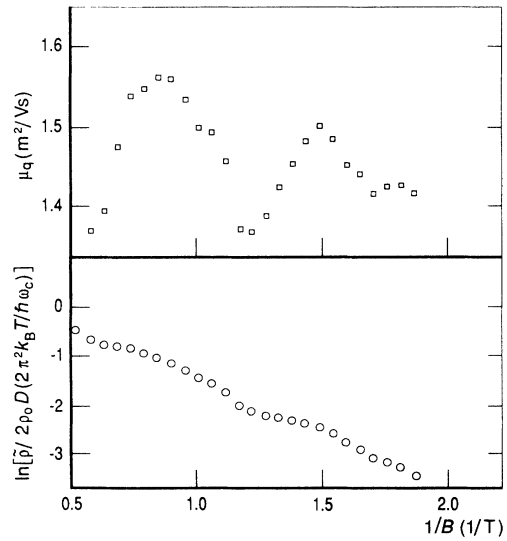

FIG. 4. Single-particle relaxation time of the lowest-subband electrons plotted as $\mu_q=e\tau_{S0}/m^*$ vs $1/B$, and the corresponding Dingle plot. Note the modulation of τ_{S0} with the second-subband fundamental frequency. Sample 1, $N_0=9.12\times10^{15}$ m^{-2} and $N_1=0.79\times10^{15}$ m^{-2}.

Analysis of the Dingle plots and the $\tau_{S0}(1/B)$ plots of sample 4 did not produce observable oscillations of τ_{S0} with the second-subband fundamental frequency, not even at temperatures well below $T=1$ K. A possible cause of the absence of the oscillations of τ_{S0} in MOCVD sample 4 is the relatively large broadening of the second-subband Landau levels suggested by the very low τ_{S1} values of this sample.

For these oscillations in τ_S several different explanations can be found in the literature.

(i) Acoustic phonon mediated intersubband scattering[14] will give rise to a multiplicative term in the magnetoresistance

$$\Delta\sigma_{xx} \propto A_{01}\sin^2\left[\frac{\pi N_0 h}{2eB}\right]\sin^2\left[\frac{\pi N_1 h}{2eB}\right], \tag{6}$$

where A_{01} is related to the strength of the intersubband scattering, and N_0 and N_1 are the subband populations. It should be noted that intersubband scattering implies a relatively large momentum transfer as $q \geq (k_{F0}-k_{F1})$, so that it is screened less effectively.

(ii) Coleridge[5] gives an alternative explanation for the intermodulation of the two series of SdH oscillations, and attributes the effect to an interplay between the (thermally) broadened Landau levels and the oscillations in the Fermi energy $E_F(B)$, which is a nonlinear function of the two sets of subband Landau levels. The intermodulation increases with Landau-level broadening and intersubband scattering rate. The absence of intermodulation in the data from sample 4 does not agree with this interpretation.

(iii) Self-consistent screening is also very important, especially in the case of dominant long-range scattering: filling factor-dependent oscillations in the screening will lead to oscillations in the single-particle relaxation time. We suggest that these oscillations contribute to the oscillations in the Dingle plots; this contribution may be expected to become weaker for increased level broadening.

The middle part of Fig. 3 shows the Dingle plot of the second-subband electrons. Here only a few points can be shown as only a few second-subband SdH extrema appear. The points with the highest Landau indices are subject to large errors, due to the fact that the thermal damping exceeds the damping by level broadening. As the second-subband carriers in sample 2 are estimated to have a Dingle temperature $T_D \leq 0.5$ K the thermal broadening exceeds the level broadening approximately by a factor of 3. Measurements at lower temperatures should be performed to get more accurate values of the second-subband Dingle temperatures.

Typical results of single-particle relaxation times and mobilities derived from the Dingle plots taken at $T\approx1.2$ K are summarized in Table II. We find, in agreement with other publications[2,3] that τ_{S1} is typically a few times bigger than τ_{S0}. Furthermore, we could not detect any positive magnetoresistance in low-field transport measurements, which should be present if the subband mobilities are different.[1] Therefore we assume that μ_1/μ_0 has a value between ≈0.7 and 1.5 as the positive magnetoresistance is smaller than $\approx1\%$. Only an average mobility

TABLE II. Single-particle relaxation times and mobilities at different carrier densities. The symbols have the following meaning: $\langle\mu\rangle$ is the average transport mobility; μ_{q0} and μ_{q1} are quantum "mobilities," equal to $e\tau_{S0}/m_0^*$ and $e\tau_{S1}/m_1^*$, respectively.

Sample	1		2		3		4
N_0 (10^{15} m^{-2})	9.12	6.36	7.40	7.55	3.9	5.1	8.2
N_1 (10^{15} m^{-2})	0.79		0.32	0.50			0.61
$\langle\mu\rangle$ (m^2/Vs)	14	53	43	47	73	75	21
μ_{q0} (m^2/Vs)	1.36	2.07	2.8	2.7	2.24	2.88	1.0
μ_{q1} (m^2/Vs)	6.8		9.7	9.4			2.9
τ_{S0} (ps)	0.54	0.83	1.13	1.07	0.90	1.15	0.40
τ_{S1} (ps)	2.7		3.9	3.8			1.16

$\langle\mu\rangle$ is determined, which is expected to be approximately equal to the lowest-subband mobility as $N_1 < 0.1N_0$ in all cases mentioned in Table II. The reason that the relaxation time τ_{S1} is longer than τ_{S0} is probably due to the fact that the second-subband electrons are further separated from the interface so that they are screened very effectively by the lowest-subband electrons and thus feel weaker potential fluctuations.[4,5,29] The τ_{S1}/τ_{S0} ratio could not be determined for sample 3 as it was not possible to extract values for τ_{S1} due to the low second-subband carrier density.

The behavior of $\langle\mu\rangle$ as a function of N_s contrasts with that of τ_{S0}: at the onset of second-subband occupancy $\langle\mu\rangle$ decreases, whereas τ_{S0} increases. This agrees with results reported by Fletcher *et al.*,[4] who concluded that both intersubband scattering and additional screening by the second-subband electrons are relevant. Screening is most effective in the case of small momentum transfers, which dominate in τ_S, while $\langle\mu\rangle$ is dominated by large momentum transfers and thus by intersubband scattering.

From the ratios between the different relaxation times we conclude that the electrons are subject predominantly to screened long-range Coulomb scattering due to the Si donors in the (Ga,Al)As. The larger distance between the second-subband wave function and the interface leads to very effective screening by the lowest-subband electrons so that its relaxation time τ_{S1} is a factor of 3 to 5 longer than τ_{S0}. However, the subband mobilities are very close to each other because of the smaller Fermi velocity of the second-subband electrons: these are subject to larger scattering angles ($\theta \propto q/k_{Fi}$).

In the data of Table II no clear relation is found between τ_{S0} and the spacer width: sample 4 has the smallest τ_{S0} but it has the same spacer width as sample 2, which has a much longer τ_{S0}. If we consider the other three more similar MBE-grown samples we see that τ_{S0} doubles if the spacer width is doubled from 5 to 10 nm, but a further doubling of the spacer to 20 nm has only a small effect on τ_{S0}. It may be concluded that sample 3 has either more effective scatterers in the δ-doping layer or that other scattering mechanisms become important. The ratio $\langle\tau_t\rangle/\tau_{S0}$ (where $e\langle\tau_t\rangle/m^* = \langle\mu\rangle$), however, is clearly dependent on the spacer width. This ratio is approximately equal to 10 for a 5-nm spacer (sample 1), between 15 and 25 for a 10-nm spacer (sample 2) and between 25 and 35 for a 20-nm spacer (sample 3). However, this dependence is weaker than the quadratic behavior suggested by the diffusion model of Uemura.[30] This difference is expected to be an effect of screening, which decreases the τ_t/τ_S ratio in the case of long-range Coulomb scattering.[25]

C. Filling factor-dependent screening in tilted fields

If an ideal 2DEG is rotated through an angle θ from the perpendicular field orientation, the only effect is that all features shift to higher field values $B_\perp = B\cos\theta$.[31] In a real 2DEG however, the parallel-field component gives rise to a diamagnetic subband shift analogous to the case of a purely parallel field.[32] Furthermore, at a fixed perpendicular field component, the spin splitting becomes stronger as it depends on the total field. At strong fields subband Landau-level coupling becomes important,[32–35] especially at field values where $r\hbar\omega_c = E_{10}$ (r is an integer referred to as the order of the subband Landau-level coupling). It should be noted that in Shubnikov–de Haas measurements we are only concerned with Landau-level degeneracies, and hence the periodicity of the oscillations depends only on $B_\perp$ (Ref. 32).

In Fig. 5 some SdH traces are shown that have been

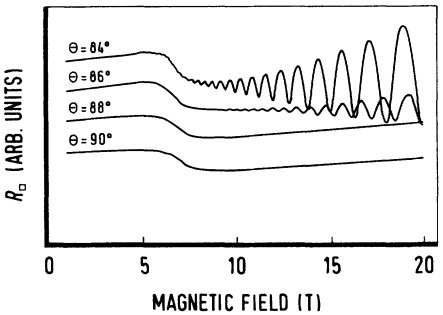

FIG. 5. Set of near-parallel-field magnetoresistance traces showing the effects of a perpendicular magnetic-field component: at low fields the resistivity increases with the perpendicular field component due to classical magnetoresistance in a 2DEG with two types of carriers of different mobility. At higher perpendicular field components SdH oscillations develop from which the single-particle relaxation time can be extracted. Sample 4, $N_s = 8.6\times10^{15}$ m^{-2}.

taken at tilt angles between 84° and 90° using sample 4. If the sample is rotated away from the parallel-field orientation $\theta=90°$ an increase of the positive magnetoresistance at low fields is observed, the depopulation structure becomes more pronounced, and SdH oscillations of growing strength are superimposed on the magnetoresistance. The positive magnetoresistance is due to the increasing perpendicular magnetic-field component, and the resulting classical positive magnetoresistance in a 2DEG with two types of carriers of different mobility.[36] When the second subband is depopulated, only one type of carrier is left and the effect disappears, so that the depopulation structure becomes more pronounced. At total fields at which the second subband is completely depopulated a (small) perpendicular field component should not cause an increase in resistivity. However, we observe a *weak* positive magnetoresistance beyond the depopulation field, also at exactly parallel field. This has been explained in Ref. 37; it is expected to become important if $\hbar\omega_{c\parallel} \geq E_{10}$.

The single-particle relaxation time is also affected by the parallel field and particularly by the second-subband depopulation. If the sample is rotated from the parallel orientation, SdH oscillations due to the perpendicular field component become resolved. At $\theta \approx 82°$ these SdH oscillations show a remarkable behavior, which is shown in Fig. 6(a) for sample 3. The amplitude of the oscillations generally increases with field, but it *decreases* in the field range where the average background magnetoresistance has a negative slope. This reflects a decrease of the single-particle relaxation time τ_{S0}, when the additional screening by the second-subband electrons disappears. In Fig. 6(b) the corresponding Dingle plot and relaxation time τ_{S0} are shown. The value of τ_{S0} has been derived from the Dingle plot using Eq. (5), where ω_c has been put equal to $eB_\perp/m^*$ and $\tau_S=\tau_S(B)$. It can be seen that τ_{S0} *decreases* when the second subband depopulates, while the negative slope of the resistivity indicates an *increase* of the transport scattering time τ_{t0}. A similar effect was discussed by Fletcher *et al.*,[2,4] who performed measurements and calculations of τ_{t0} and τ_{S0} as a function of carrier density in a range where the second subband starts to be populated, and found an increase of τ_{S0} at the onset of metallic screening by second-subband "extended" electrons (see also the preceding section of this paper). In Table III some values of τ_{S0} are shown that have been extracted from the straight parts of the Dingle plots,[26] (i.e., at low parallel fields and parallel fields beyond the depopulation field), for samples 2, 3, and 4. The Shubnikov–de Haas oscillations superposed on the depopulation curve were not sufficiently well resolved to allow a similar analysis for sample 1. It appears that the relative difference tends to increase with the single-particle relaxation time, which means that the screening by the second-subband electrons tends to be more effective as the quantum lifetimes increase. This can be an effect of the spacer width: screening by the second-subband electrons becomes more effective as the spacer width increases. Also the tilt angle has some influence, as it determines the relative importance of Landau-level formation in the second subband, which affects the screening properties of the corresponding carriers. As soon as the SdH oscillations start to be modulated by the second-subband Landau levels, oscillations in $\tau_{S0}(B)$ appear. These are *not* strictly periodic in $1/B$ as the second-subband carrier density decreases with field due to the large parallel component.

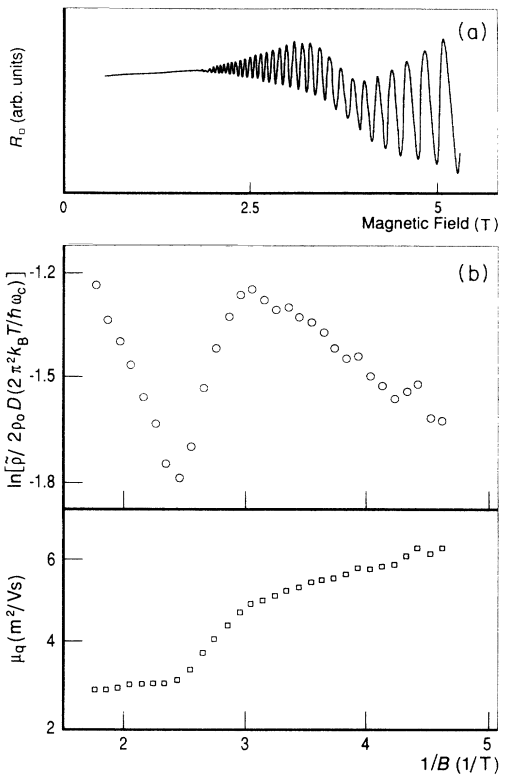

FIG. 6. Shubnikov–de Haas signal (a), and corresponding Dingle plot and quantum mobility (b) vs $1/B_\perp$; the tilt angle is 82°. Note the sharp bends that are due to the change of the single-particle relaxation time as a result of the change of additional screening by the second subband. Sample 3, $N_s=4.93\times10^{15}$ m^{-2}.

D. Depopulation curves in parallel magnetic field

In this subsection we discuss some additional features of the depopulation curves. From linear extrapolation of the magnetoresistance in the depopulation curves taken at parallel magnetic field below and above the transition, and approximating the transition by a straight line with the slope at the midpoint of the transition, we have evaluated the shift in resistivity $\Delta R_\square$ and the transition width $\Delta B_{\rm dep}$ around the depopulation field $B_{\rm dep}$. The step in the resistivity is attributed completely to intersubband scattering. $\rho_{xx}=R_\square$ at low temperatures is proportional to the inverse of the transport scattering time τ_t, and we can relate the scattering times using the following equation (the scattering processes are assumed to be independent, so that they obey Matthiessen's rule[24]):

$$\frac{1}{\tau_t}=\frac{1}{\tau_{\rm intra}}+\frac{1}{\tau_{\rm inter}} . \tag{7}$$

TABLE III. Single-particle relaxation times expressed in terms of quantum mobilities $\mu_q = e\tau_S/m^*$, extracted from tilted-field traces taken at large fixed angles. The values have been extracted from two series of successive SdH amplitudes corresponding to parallel-field ranges below and beyond the depopulation structure, respectively.

Sample	2		3		4	
N_0 (10^{15} m^{-2})	7.40	7.55	4.9	5.3	8.0	8.0
N_1 (10^{15} m^{-2})	0.32	0.50	≈0.2	≈0.2	0.6	0.6
θ (°)	83	85	82	84	80	82
$\langle\mu_q\rangle$ (high $B_\parallel$) (m^2/Vs)	3.7	2.3	3.8	4.6	1.0	1.0
$\langle\mu_q\rangle$ (low $B_\parallel$) (m^2/Vs)	≈4.5	3.5	8	6.3	1.45	1.35

As $R_\square = R_{\square,\text{intra}} + \Delta R_\square$ (where $R_{\square,\text{intra}}$ is the resistivity at $B_\parallel$ just above the depopulation transition), it follows that

$$\Delta R_\square = \frac{m^*}{Ne^2\tau_{\text{inter}}} . \tag{8}$$

The results for B_{dep} of samples 1 and 2 were shown in Fig. 2; Fig. 7 compiles the corresponding results of the two contributions to the total scattering rate $1/\tau_{\text{intra}}$ and $1/\tau_{\text{inter}}$. The intrasubband relaxation time τ_{intra} is proportional to $1/R_{\square,\text{intra}}$ just above the depopulation field when the effect of second-subband population has disappeared. In Fig. 7 it can be seen that $1/\tau_{\text{intra}}$ decreases with increasing N_s: this is expected to be a result of enhanced screening. The intersubband scattering rate $1/\tau_{\text{inter}}$ is proportional to $\Delta R_\square$, and is seen to increase with N_s. The intersubband scattering rate $1/\tau_{\text{inter}}$ shows a strong decrease with increasing mobility (i.e., spacer width). This can be understood as follows: intersubband scattering represents an additional scattering channel with momentum transfer $q \geq (k_{F0} - k_{F1})$. The Fourier transform $U(\mathbf{q})$ of the scattering potential $U(\mathbf{r})$ strongly decreases with spacer width for large q so that $1/\tau_{\text{inter}}$ decreases.

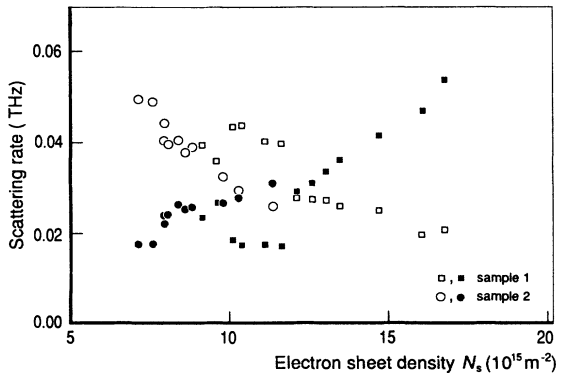

FIG. 7. Intersubband scattering rate (solid symbols) and intrasubband scattering rate (open symbols) determined from the parallel-field depopulation curve. Sample 1; □, scaled down $\frac{1}{5}\tau^{-1}$; sample 2, ○, to scale.

Furthermore we see that $1/\tau_{\text{inter}}$ goes up with increasing N_s. As this behavior is the strongest in sample 1, which has the smallest spacer width, we expect that it is a result of the fact that the subband wave functions are pushed toward the interface when the density increases. This would lead to an increase of ionized impurity scattering especially for large momentum transfers.

For each of the four samples studied we have observed a significant decrease of the relative width $\Delta B_{\text{dep}}/B_{\text{dep}}$ with increasing carrier density N_s and with increasing mobility. With a parabolic relation between $B_\parallel$ and $(E_F - E_1)$,[16] one can estimate the width of the depopulation structure ΔB_{dep} qualitatively. The behavior of the product of $N_1(B_\parallel = 0)$ and $\Delta B_{\text{dep}}/B_{\text{dep}}$ found is the same as the variations with N_s and μ of the level width (given by the lifetime broadening $\Gamma = \hbar/\tau_S$) of the Landau levels of the second subband.

IV. SUMMARY AND CONCLUSIONS

We have studied the magnetotransport properties of four different high-carrier-density GaAs-(Ga,Al)As heterojunctions, both in perpendicular and in tilted fields. We found a big influence of intersubband scattering and oscillatory screening on the experimental results.

From the field dependence of the amplitudes of both SdH periodicities we found that the single-particle relaxation times of the electrons in the lowest and first excited subbands have a ratio $\tau_{S1}/\tau_{S0} \approx 3$. A study of the field dependence of τ_{S0} revealed oscillations that are attributed to nonlinear intersubband scattering and oscillatory screening by the Landau levels of the second subband. In one of the samples (MOCVD sample 4), such oscillations were not found, indicating that the effect is closely related to the level width and sample composition.

Parallel-field depopulation fields are found to agree with the model of Reisinger and Koch[19] after some illumination. This indicates an accumulation-layer-like behavior of the samples.

Measurements of the lowest-subband SdH amplitudes at large tilt angles ($\theta \geq 80°$) showed that τ_{S0} decreases when the second subband depopulates; this confirms the

importance of additional screening of long-range scatterers by second-subband electrons. Occupation of the second subband thus leads to the onset of intersubband scattering, which decreases the mobility, but it also leads to additional screening, which enhances the single-particle relaxation time in spite of the onset of intersubband scattering.

ACKNOWLEDGMENTS

This work was supported by the Stichting voor Fundamenteel Onderzoek der Materie (FOM) with financial help from the Nederlandse Organisatie voor Wetenschappelijk Onderzoek (NWO), and by the SCIENCE program of the European Communities.

---

*Present address: Royal Dutch/Shell Exploration and Production Laboratory, NL-2280 AB Rijswijk, The Netherlands.

†Present address: Clarendon Laboratory, University of Oxford, Oxford OX1 3PU, United Kingdom.

[1]H. van Houten, J. G. Williamson, M. E. I. Broekaart, C. T. Foxon, and J. J. Harris, Phys. Rev. B **37**, 2756 (1988).

[2]R. Fletcher, E. Zaremba, M. D'Iorio, C. T. Foxon, and J. J. Harris, Phys. Rev. B **38**, 7866 (1988).

[3]T. P. Smith III, F. F. Fang, U. Meirav, and M. Heiblum, Phys. Rev. B **38**, 12744 (1988).

[4]R. Fletcher, E. Zaremba, M. D'Iorio, C. T. Foxon, and J. J. Harris, Phys. Rev. B **41**, 10649 (1990).

[5]P. T. Coleridge, Semicond. Sci. Technol. **5**, 961 (1990).

[6]G. Gobsch, D. Schulze, and G. Paasch, Phys. Rev. B **38**, 10943 (1988).

[7]T. Ando and Y. Murayama, J. Phys. Soc. Jpn. **54**, 1519 (1985).

[8]R. Lassnig and E. Gornik, Solid State Commun. **47**, 959 (1983).

[9]S. Das Sarma, Phys. Rev. B **23**, 4592 (1981).

[10]The MBE samples were grown at the Cavendish Laboratory, Cambridge, U.K.: sample 1 was denoted as A227, sample 2 as A232, and sample 3 as A233.

[11]A. Zrenner, F. Koch, R. L. Williams, R. A. Stradling, K. Ploog, and G. Weimann, Semicond. Sci. Technol. **3**, 1203 (1988).

[12]The MOCVD sample was grown at the Laboratoire d'Electronique et de Physique Appliquée, Limeil-Brevannes, France: sample 4 was denoted as E518.

[13]B. A. Joyce, Rep. Prog. Phys. **48**, 1637 (1985).

[14]D. R. Leadley, R. J. Nicholas, J. J. Harris, and C. T. Foxon, Semicond. Sci. Technol. **4**, 885 (1989).

[15]E. F. Schubert, K. Ploog, H. Dämbkes, and K. Heime, Appl. Phys. **33A**, 63 (1984); H. L. Stormer, A. C. Gossard, W. Wiegmann, and K. Baldwin, Appl. Phys. Lett. **39**, 912 (1981); A. Kastalsky, and J. C. M. Hwang, *ibid.* **44**, 333 (1984).

[16]T. Ando, J. Phys. Soc. Jpn. **51** 3893 (1982); **51**, 3900 (1982).

[17]J. J. Harris, D. E. Lacklison, C. T. Foxon, F. M. Selten, A. M. Suckling, R. J. Nicholas, and K. W. J. Barnham, Semicond. Sci. Technol. **2**, 783 (1987).

[18]K. Ensslin, D. Heitmann, and K. Ploog, Phys. Rev. B **39**, 10879 (1989).

[19]H. Reisinger and F. Koch, Surf. Sci. **170**, 397 (1986).

[20]F. Nasir, J. Singleton, and R. J. Nicholas, Semicond. Sci. Technol. **3**, 654 (1988).

[21]D. J. Newson, K.-F. Berggren, M. Pepper, H. W. Myron, G. J. Davies, and E. G. Scott, J. Phys. C **19**, 403 (1986).

[22]D. G. Cantrell and P. N. Butcher, J. Phys. C **18**, 5111 (1985).

[23]K. Seeger, *Semiconductor Physics,* Springer Series in Solid State Sciences Vol. 40 (Springer-Verlag, Berlin, 1973).

[24]N. W. Ashcroft and N. D. Mermin, *Solid State Physics* (Holt, Rinehart and Winston, New York, 1976).

[25]J. P. Harrang, R. J. Higgins, R. K. Goodall, P. R. Jay, M. Laviron, and P. Delescluse, Phys. Rev. B **32**, 8126 (1985).

[26]P. T. Coleridge, R. Stoner, and R. Fletcher, Phys. Rev. B **39**, 1120 (1989).

[27]T. Ando, A. B. Fowler, and F. Stern, Rev. Mod. Phys. **54**, 437 (1982).

[28]M. Watts, I. Auer, R. J. Nicholas, J. J. Harris, and C. T. Foxon, in *High Magnetic Fields in Semiconductor Physics III,* edited by G. Landwehr, Springer Series in Solid State Sciences Vol. 101 (Springer Verlag, Berlin, 1992), p. 581.

[29]T. P. Smith III and F. F. Fang, Phys. Rev. B **37**, 4303 (1988).

[30]Y. Uemura, *Proceedings of the 12th International Conference on the Physics of Stuttgart, 1974, edited by M. H. Pilkuhn* (Teubner, Stuttgart, 1974), p. 665.

[31]F. Stern and W. E. Howard, Phys. Rev. **163**, 816 (1967).

[32]T. Ando, Phys. Rev. B **19**, 2106 (1979).

[33]Z. Schlesinger, J. C. M. Hwang, and S. J. Allen, Phys. Rev. Lett. **50**, 2098 (1983).

[34]G. L. J. A. Rikken, H. Sigg, C. J. G. M. Langerak, H. W. Myron, J. A. A. J. Perenboom, and G. Weimann, Phys. Rev. B **34**, 5590 (1986).

[35]A. D. Wieck, F. Thiele, U. Merkt, and K. Ploog, Phys. Rev. B **39**, 3785 (1989).

[36]M. J. Kane, N. Apsley, D. A. Anderson, L. L. Taylor, and T. Kerr, J. Phys. C **18**, 5629 (1985).

[37]H. Tang and P. N. Butcher, J. Phys. C **21**, 3313 (1988).